Research Article

Milica Marković*

Dynamical properties of two-diffusion SIR epidemic model with Markovian switching

https://doi.org/10.1515/math-2024-0123
received April 17, 2024; accepted December 22, 2024

Abstract: Infectious diseases still remain one of the major causes of death worldwide, despite the fact that various treatments, such as antibiotics, antiviral drugs, and vaccines for some diseases, are more available to people. Factors such as drug resistance, lack of access to health care, and environmental changes contribute to their persistence and spread. Motivated by this fact, in this study, the stochastic susceptible-infectious-recovered (SIR) epidemiological model with treatment and non-linear incidence rate is extended, by introducing coloured noise, to model which takes into account the seasonal nature of the disease, as well as the fact that the disease is constantly changing through mutations, which leads to the appearance of new disease strains. For the model formulated in this way, we first prove the existence and uniqueness of the global positive solution. Then, we provide conditions under which the disease persists in the population, as well as sufficient conditions for the disease to die out. The theoretical results of the current study are validated by numerical simulations. For that purpose, we use data on the spread of the Ebola epidemic in Sierra Leone and the coronavirus disease 2019 (COVID-19) pandemic in Pakistan. Both theoretical and numerical results can lead us to conclusion that our model represents the solid research base for further investigation in the field of epidemiological modelling.

Keywords: existence and uniqueness, extinction, Markov chain, persistence in mean, SIR model, stochastic trajectories

MSC 2020: 60H10, 92D25, 93E15

1 Introduction and motivation

The mathematical approach in epidemiology is related to the study of the spread of infectious diseases in a population. These diseases can be transmitted from animals to humans or from humans to humans through physical contact with an infected person or animal, as well as through the contact with person or animal that carry the virus, so that they can transmit it to someone else, even though they are not infected themselves. The infection can also be transmitted through air, water, soil, etc. Given that experiments in the field of epidemiology are not possible due to numerous ethical and technical reasons, it turned out that mathematical models are a very useful tool that can be used to predict the outbreak of epidemics, but also to measure the effects of various preventive measures on their control and suppression. Different types of the diseases are modelled by different epidemiological models. In mathematical literature, there are many studies that consider deterministic models that describe the spread of a disease in a large population (see [1–3], for instance). These models are mainly based on the so-called mass action law, so it is assumed that people within a population mix homogeneously, which in fact means that they come into contact independently of each other and everyone has an equal chance to encounter any other individual. The classic susceptible-infectious-recovered (SIR) epidemiological model is one of the most commonly implemented models where the total

* **Corresponding author: Milica Marković,** Faculty of Mechanical Engineering, University of Niš, Aleksandra Medvedeva 14, 18000 Niš, Serbia, e-mail: milica.milunovic@masfak.ni.ac.rs

population at time t denoted by $N(t)$ is divided into three compartments: "susceptible" $S(t)$, "infected" $I(t)$, and "recovered" $R(t)$. It is used to model diseases after which the recovered patients acquire permanent immunity. It was initially proposed and studied by Kermack and McKendrick in a set of three articles from 1927, 1932, and 1933. Because of their importance to the field of theoretical epidemiology, these articles were republished [4–6]. The model is of the form

$$\begin{aligned} \frac{\mathrm{d}S}{\mathrm{d}t} &= -\beta IS, \\ \frac{\mathrm{d}I}{\mathrm{d}t} &= \beta IS - \gamma I, \\ \frac{\mathrm{d}R}{\mathrm{d}t} &= \gamma I, \end{aligned} \tag{1}$$

with initial condition $S(0) = S_0$, $I(0) = I_0$, $R(0) = R_0$, while β is the transmission rate and γ natural recovery rate.

In [1], the authors constructed the SIR epidemiological model using a nonlinear saturated incidence rate given by $\frac{\beta IS}{1+kI}$, unlike the incidence rate in (1), βIS. This is great improvement because the incidence rate of such form does not allow unlimited number of contacts, and the term $\frac{1}{1+kI}$ represents precautionary measures for individuals with a compromised immune system, making them more susceptible to infection. In addition to precautionary measures, treatment is another method to prevent and control the spread of infectious diseases. Zhou and Fan [1] considered a nonlinear saturated treatment function expressed as $\frac{\alpha I}{\omega+I}$ and investigated how limited medical resources and their supply efficiency affect the transmission of infectious diseases. The model is represented by a system of ordinary differential equations of the form

$$\begin{aligned} \frac{\mathrm{d}S}{\mathrm{d}t} &= \Lambda - \frac{\beta IS}{1+kI} - \mu S, \\ \frac{\mathrm{d}I}{\mathrm{d}t} &= \frac{\beta IS}{1+kI} - (\mu+\varepsilon+\gamma)I - \frac{\alpha I}{\omega+I}, \\ \frac{\mathrm{d}R}{\mathrm{d}t} &= \gamma I + \frac{\alpha I}{\omega+I} - \mu R, \end{aligned} \tag{2}$$

with the initial conditions $S(0) = S_0$, $I(0) = I_0$, $R(0) = R_0$, while biological interpretation of the parameters is described in Table 1.

Since people within the population do not meet completely by chance, but each person has a certain circle of people with whom he/she is in daily contact, the assumption of homogeneous mixing in deterministic models is not realistic. That is why, stochastic models represent the more appropriate way of modelling epidemics than their deterministic analogues. In the literature, there are many studies that consider dynamics of the stochastic epidemiological models [7–13]. Due to the fact that almost all diseases have an incubation

Table 1: Biological interpretation of the variables and parameters of model (2)

$S(t)$	The number of susceptible people
$I(t)$	The number of infected people
$R(t)$	The number of recovered people
Λ	The recruitment rate of the population
β	The transmission rate
$\frac{1}{1+kI}$	The precautionary measures
μ	The natural death rate
ε	The mortality rate related to the disease
γ	The natural recovery rate
α	The maximum medical resources per unit of time
ω	The half-saturation constant

period, many authors naturally assumed that epidemiological models with time delay are more suitable to analyse the spread of the infectious diseases (see [14–16], among others).

Based on model (2), Milunović and Krstić [12] the authors constructed stochastic SIR epidemiological model of the form

$$\begin{aligned}
\mathrm{d}S(t) &= \left(\Lambda - \frac{\beta I(t)S(t)}{1+kI(t)} - \mu S(t)\right)\mathrm{d}t - \frac{\sigma_1 I(t)S(t)}{1+kI(t)}\mathrm{d}B_1(t),\\
\mathrm{d}I(t) &= \left(\frac{\beta I(t)S(t)}{1+kI(t)} - (\mu+\varepsilon+\gamma)I(t) - \frac{\alpha I(t)}{\omega+I(t)}\right)\mathrm{d}t + \frac{\sigma_1 I(t)S(t)}{1+kI(t)}\mathrm{d}B_1(t) - \frac{\sigma_2 I(t)}{\omega+I(t)}\mathrm{d}B_2(t),\\
\mathrm{d}R(t) &= \left(\gamma I(t) + \frac{\alpha I(t)}{\omega+I(t)} - \mu R(t)\right)\mathrm{d}t + \frac{\sigma_2 I(t)}{\omega+I(t)}\mathrm{d}B_2(t),
\end{aligned} \tag{3}$$

with the initial conditions $S(0) = S_0$, $I(0) = I_0$, $R(0) = R_0$, where σ_1 and σ_2 are the real constants, and $B_1(t)$ and $B_2(t)$ are two independent standard Brownian motions defined on complete probability space $(\Omega, \mathcal{F}, P)$ with the filtration $\{\mathcal{F}_t\}_{t\geq 0}$, satisfying the usual conditions (it is right continuous and increasing, while $\mathcal{F}_0$ contains all P-null sets), while other parameters are defined as in Table 1. For model (3), the authors showed the existence and uniqueness of the global positive solution and that the solution remains in the set

$$\Gamma = \left\{(S(t), I(t), R(t)) \in \mathbb{R}_+^3 : S(t) + I(t) + R(t) < \frac{\Lambda}{\mu}\right\},$$

provided that $(S_0, I_0, R_0) \in \Gamma$. Moreover, they proved that the solution admits the unique stationary distribution, which means that the system is stochastically weak stabile, i.e. the disease will prevail in the population in long time, and then, they gave the sufficient conditions under which the disease-free equilibrium of system (3) is pth moment and almost surely exponentially stable, as well as the conditions under which extinction of the disease occurs.

Population dynamics is often affected by various types of external environmental noises, such as the changes in weather, temperature, and climate. Since these fluctuations may cause dramatic changes in some important parameters of infectious diseases (e.g., transmission rate, death rate, recovery rate), they are generally described as switching between two or more regimes of the environment. In the literature, the switching can be generally illustrated as a continuous-time Markov chain, which drives the changes of the main parameters of population and epidemiological models with state switchings of homogeneous Markov chain [17–26]. With that motivation, we introduce coloured or telegraphic noise in (3), which will be represented by right-continuous Markov chain $\{\vartheta(t), t \geq 0\}$, defined on complete probability space $(\Omega, \mathcal{F}, P)$ with the filtration $\{\mathcal{F}_t\}_{t\geq 0}$, independent of Brownian motions $B_1(t)$, $B_2(t)$, and taking values in a finite space $\mathcal{S} = \{1, 2, \ldots, N\}$. Hence, model (3) becomes

$$\begin{aligned}
\mathrm{d}S(t) &= \left(\Lambda(\vartheta(t)) - \frac{\beta(\vartheta(t))I(t)S(t)}{1+k(\vartheta(t))I(t)} - \mu(\vartheta(t))S(t)\right)\mathrm{d}t - \frac{\sigma_1(\vartheta(t))I(t)S(t)}{1+k(\vartheta(t))I(t)}\mathrm{d}B_1(t),\\
\mathrm{d}I(t) &= \left(\frac{\beta(\vartheta(t))I(t)S(t)}{1+k(\vartheta(t))I(t)} - (\mu(\vartheta(t)) + \varepsilon(\vartheta(t)) + \gamma(\vartheta(t)))I(t) - \frac{\alpha(\vartheta(t))I(t)}{\omega(\vartheta(t))+I(t)}\right)\mathrm{d}t + \frac{\sigma_1(\vartheta(t))I(t)S(t)}{1+k(\vartheta(t))I(t)}\mathrm{d}B_1(t)\\
&\quad - \frac{\sigma_2(\vartheta(t))I(t)}{\omega(\vartheta(t))+I(t)}\mathrm{d}B_2(t),\\
\mathrm{d}R(t) &= \left(\gamma(\vartheta(t))I(t) + \frac{\alpha(\vartheta(t))I(t)}{\omega(\vartheta(t))+I(t)} - \mu(\vartheta(t))R(t)\right)\mathrm{d}t + \frac{\sigma_2(\vartheta(t))I(t)}{\omega(\vartheta(t))+I(t)}\mathrm{d}B_2(t),
\end{aligned} \tag{4}$$

with the initial conditions $S(0) = S_0$, $I(0) = I_0$, $R(0) = R_0$, $\vartheta(0) \in \mathcal{S}$, and for any $\iota \in \mathcal{S}$, coefficients $\Lambda(\iota)$, $\beta(\iota)$, $k(\iota)$, $\mu(\iota)$, $\varepsilon(\iota)$, $\gamma(\iota)$, $\alpha(\iota)$, $\omega(\iota)$, $\sigma_1(\iota)$, and $\sigma_2(\iota)$ are positive. The infinitesimal generator matrix $Q = [\lambda_{\iota\kappa}]_{N\times N}$ is defined by

$$P\{\vartheta(t+\Delta) = \kappa | \vartheta(t) = \iota\} = \begin{cases} \lambda_{\iota\kappa}\Delta + o(\Delta), & \iota \neq \kappa,\\ 1 + \lambda_{\iota\iota}\Delta + o(\Delta), & \iota = \kappa, \end{cases}$$

where $\lambda_{\iota\kappa} \geq 0$ is the transition rate from state ι to κ if $\iota \neq \kappa$ while $\lambda_{\iota\iota} = -\sum_{\kappa \neq \iota} \lambda_{\iota\kappa}$. We assume that $\lambda_{\iota\kappa} > 0$ for $\iota, \kappa = 1, 2, \ldots, N$ with $\iota \neq \kappa$. This assumption provides that the Markov chain $\vartheta(t)$ is irreducible, i.e. there exists a unique stationary distribution $\pi = (\pi_\iota)_{1\times N}$ such that $\pi Q = 0$, $\sum_{\iota=1}^{N} \pi_\iota = 1$ and $\pi_\iota > 0$ for any $\iota \in \mathcal{S}$.

For discussion convenience, define $\hat{\rho} = \max_{\iota\in\mathcal{S}} \rho(\iota)$ and $\check{\rho} = \min_{\iota\in\mathcal{S}} \rho(\iota)$.

As it was already mentioned, there are many articles in the mathematical literature dealing with the dynamical behaviour of SIR epidemiological models with or without Markovian switching. Since we present a detailed analysis of a stochastic SIR epidemiological model with treatment, non-linear incidence rate, two diffusions, and Markovian switching, we regard this study as a generalization of the articles that can be found in literature. More precisely, we can consider articles [18,25] as a special case of our model, because in the study [18], there is no treatment function and second diffusion, i.e. $\alpha = 0$ and $\sigma_2 = 0$. This is a shortcoming of [18,25] as it ignores the impact of the environment on limited medical resources, especially considering the coronavirus disease 2019 (COVID-19) pandemic, where the unpredictability of this parameter has been shown. Also, the recent catastrophic earthquake in Turkey and Syria, which destroyed many hospitals and killed many medical workers, proves the importance of the parameter σ_2 in our model. Furthermore, compared to the extinction results obtained in [18], we provide the weaker conditions for model parameters, which is improvement of the existing results.

For all epidemiological models, the basic reproduction number is a very important quantity, which describes the dynamics of the disease. It represents the average number of secondary infections that single infected person may generate in a susceptible population. For model (2), the basic reproduction number is computed in [1] by the next-generation method, and it is given by

$$\mathcal{R}_0 = \frac{\beta\Lambda}{\mu\left(\mu + \varepsilon + \gamma + \frac{\alpha}{\omega}\right)}. \tag{5}$$

In general, it is more difficult to determine the basic reproduction number for stochastic models. For model (4), we will show that the quantity $\mathcal{R}_0^s$ defined by

$$\mathcal{R}_0^s = \frac{\sum_{\iota=1}^{N}\pi_\iota\beta(\iota)\sum_{\iota=1}^{N}\pi_\iota\Lambda(\iota)}{\mathcal{N}\sum_{\iota=1}^{N}\pi_\iota\mu(\iota)} - \frac{\sum_{\iota=1}^{N}\pi_\iota\Lambda^2(\iota)\sum_{\iota=1}^{N}\pi_\iota\sigma_1^2(\iota)}{2\mathcal{N}\sum_{\iota=1}^{N}\pi_\iota\mu^2(\iota)} - \frac{1}{2\mathcal{N}}\sum_{\iota=1}^{N}\pi_\iota\frac{\sigma_2^2(\iota)}{\omega^2(\iota)}, \tag{6}$$

where

$$\mathcal{N} = \sum_{\iota=1}^{N}\pi_\iota\left(\mu(\iota) + \varepsilon(\iota) + \gamma(\iota) + \frac{\alpha(\iota)}{\omega(\iota)}\right), \tag{7}$$

and model parameters satisfy the condition $\mathcal{R}_0^s > 0$, i.e.

$$\frac{\sum_{\iota=1}^{N}\pi_\iota\Lambda^2(\iota)\sum_{\iota=1}^{N}\pi_\iota\sigma_1^2(\iota)}{\sum_{\iota=1}^{N}\pi_\iota\mu^2(\iota)} + \sum_{\iota=1}^{N}\pi_\iota\frac{\sigma_2^2(\iota)}{\omega^2(\iota)} < \frac{2\sum_{\iota=1}^{N}\pi_\iota\beta(\iota)\sum_{\iota=1}^{N}\pi_\iota\Lambda(\iota)}{\sum_{\iota=1}^{N}\pi_\iota\mu(\iota)},$$

determines the extinction and persistence in mean of the disease. It is easy to see that $\mathcal{R}_0^s$ becomes $\mathcal{R}_0$ when there is no white and coloured noise.

The rest of this article is organized as follows. In the next section, we prove that model (4) has a unique global positive solution for any initial positive value. In Section 3, we give sufficient conditions under which the disease is persistent in mean. Results on extinction are presented in Section 4. In Section 5, we illustrate the theoretical results from Sections 3 and 4 by using real data for Ebola outbreak in Sierra Leone and COVID-19 pandemic in Pakistan. The obtained simulations show that the model (4) predicts the course of the disease well, and can be used for all diseases and disease variants in which permanent immunity is acquired. We close the study with a conclusion section.

2 Existence and uniqueness of global positive solution

From a biological point of view, it is important to see whether the solution of (4) is global and positive. Consider the set

$$\mathcal{G} = \left\{(S(t), I(t), R(t)) \in \mathbb{R}^3_+ : S(t) + I(t) + R(t) < \frac{\hat{\Lambda}}{\check{\mu}}\right\}. \tag{8}$$

Based on Theorem 3.1 in [12], we present the following theorem.

Theorem 2.1. *There is a unique continuous time, Markovian global solution* $(S(t), I(t), R(t))$ *of system* (4)*, on* $t \geq 0$ *with initial condition* $(S_0, I_0, R_0, \vartheta(0)) \in \mathcal{G} \times \mathcal{S}$*. This solution is invariant with respect to* $\mathcal{G}$ *with probability one.*

Proof. Since the coefficients of system (4) are locally Lipschitz continuous, for any initial value, there exists a unique local solution $(S(t), I(t), R(t))$ on $t \in [0, \tau(\mathcal{G}))$, where $\tau(\mathcal{G})$ represents the explosion time. To show that this solution is global, we need to prove that $\tau(\mathcal{G}) = \infty$ a.s. Let

$$\mathcal{G}_n = \left\{(S(t), I(t), R(t)) : e^{-n} < S(t) < \frac{\hat{\Lambda}}{\check{\mu}} - e^{-n}, e^{-n} < I(t) < \frac{\hat{\Lambda}}{\check{\mu}} - e^{-n}, e^{-n} < R(t) < \frac{\hat{\Lambda}}{\check{\mu}} - e^{-n},\right.$$
$$\left. S(t) + I(t) + R(t) < \frac{\hat{\Lambda}}{\check{\mu}}\right\},$$

for $n \in \mathbb{N}$. System (4) has a unique solution up to stopping time $\tau(\mathcal{G}_n)$.

Let us define a C^2-function

$$V(S(t), I(t), R(t)) = S(t) - \ln S(t) + I(t) - \ln I(t) + R(t) + \frac{\hat{\Lambda}}{\check{\mu}} - S(t) - \ln\left(\frac{\hat{\Lambda}}{\check{\mu}} - S(t)\right),$$

on set $\mathcal{G}$. Nonnegativity of this function can be seen from inequality $u - 1 - \ln u \geq 0$ for any $u > 0$, and we have $V(S(t), I(t), R(t)) \geq 3$ for $(S(t), I(t), R(t)) \in \mathcal{G}$.

Application of differential operator L on V yields

$$\begin{aligned} LV = {} & \frac{\Lambda(\vartheta(t))}{\frac{\hat{\Lambda}}{\check{\mu}} - S(t)} - \frac{\mu(\vartheta(t))S(t)}{\frac{\hat{\Lambda}}{\check{\mu}} - S(t)} - \frac{\beta(\vartheta(t))I(t)S(t)}{(\frac{\hat{\Lambda}}{\check{\mu}} - S(t))(1 + k(\vartheta(t))I(t))} - \frac{\Lambda(\vartheta(t))}{S(t)} \\ & + \frac{\beta(\vartheta(t))I(t)(1 + S(t))}{1 + k(\vartheta(t))I(t)} - (\mu(\vartheta(t)) + \varepsilon(\vartheta(t)))I(t) - \frac{\beta(\vartheta(t))S(t)}{1 + k(\vartheta(t))I(t)} \\ & + 2\mu(\vartheta(t)) + \varepsilon(\vartheta(t)) + \gamma(\vartheta(t)) + \frac{\alpha(\vartheta(t))}{\omega(\vartheta(t)) + I(t)} - \mu(\vartheta(t))R(t) + \frac{\sigma_1^2(\vartheta(t))I(t)^2}{2(1 + k(\vartheta(t))I(t))^2} \\ & + \frac{\sigma_1^2(\vartheta(t))I(t)^2S(t)^2}{2(\frac{\hat{\Lambda}}{\check{\mu}} - S(t))^2(1 + k(\vartheta(t))I(t))^2} + \frac{\sigma_1^2(\vartheta(t))S(t)^2}{2(1 + k(\vartheta(t))I(t))^2} + \frac{\sigma_2^2(\vartheta(t))}{2(\omega(\vartheta(t)) + I(t))^2}, \end{aligned}$$

which implies that

$$\begin{aligned} LV \leq {} & \frac{\Lambda(\vartheta(t))}{\frac{\hat{\Lambda}}{\check{\mu}} - S(t)} - \frac{\mu(\vartheta(t))S(t)}{\frac{\hat{\Lambda}}{\check{\mu}} - S(t)} + \frac{\beta(\vartheta(t))I(t)(1 + S(t))}{1 + k(\vartheta(t))I(t)} + 2\mu(\vartheta(t)) + \varepsilon(\vartheta(t)) + \gamma(\vartheta(t)) + \frac{\alpha(\vartheta(t))}{\omega(\vartheta(t)) + I(t)} \\ & + \frac{\sigma_1^2(\vartheta(t))I(t)^2}{2(1 + k(\vartheta(t))I(t))^2} + \frac{\sigma_1^2(\vartheta(t))I(t)^2S(t)^2}{2(I(t) + R(t))^2(1 + k(\vartheta(t))I(t))^2} + \frac{\sigma_1^2(\vartheta(t))S(t)^2}{2(1 + k(\vartheta(t))I(t))^2} + \frac{\sigma_2^2(\vartheta(t))}{2(\omega(\vartheta(t)) + I(t))^2} \\ \leq {} & \frac{\hat{\Lambda}}{\frac{\hat{\Lambda}}{\check{\mu}} - S(t)} - \frac{\check{\mu}S(t)}{\frac{\hat{\Lambda}}{\check{\mu}} - S(t)} + \frac{\hat{\beta}}{\check{k}}(1 + S(t)) + 2\hat{\mu} + \hat{\varepsilon} + \hat{\gamma} + \frac{\hat{\alpha}}{\check{\omega}} + \frac{\hat{\sigma}_1^2}{2\check{k}^2} + \hat{\sigma}_1^2(S(t))^2 + \frac{\hat{\sigma}_2^2}{2\check{\omega}^2} \end{aligned}$$

$$= \frac{\hat{\beta}}{\check{k}}\left(1 + \frac{\hat{\Lambda}}{\check{\mu}}\right) + 3\hat{\mu} + \hat{\varepsilon} + \hat{\gamma} + \frac{\hat{\alpha}}{\check{\omega}} + \frac{\hat{\sigma}_1^2}{2\check{k}^2} + \frac{\hat{\sigma}_1^2\hat{\Lambda}^2}{\check{\mu}^2} + \frac{\hat{\sigma}_2^2}{2\check{\omega}^2} \coloneqq 3c,$$

where we used the fact $S(t) + I(t) + R(t) < \frac{\hat{\Lambda}}{\check{\mu}}$ and c is a positive constant.

The rest of the proof is similar to the proof of Theorem 3.1 in [12] and therefore is omitted. □

3 Persistence in mean

In this section, we consider persistence in mean for model (4). From the epidemiological point of view, it is not desirable property because it indicates that the disease prevails in population. The definition of persistence in mean may be found in [8], for example.

Definition 3.1. Stochastic system (4) is said to be persistent in mean if

$$\liminf_{t\to\infty} \frac{1}{t}\int_0^t S(\tau)\mathrm{d}\tau > 0, \quad \liminf_{t\to\infty} \frac{1}{t}\int_0^t I(\tau)\mathrm{d}\tau > 0, \quad \liminf_{t\to\infty} \frac{1}{t}\int_0^t R(\tau)\mathrm{d}\tau > 0, \quad a.s.,$$

for any positive solutions $(S(t), I(t), R(t))$ of system (4).

To facilitate the discussion, we define

$$\mathcal{R}_1^s = \frac{\check{\beta}}{\hat{\mu}\mathcal{N}}\sum_{\iota=1}^N \pi_\iota \Lambda(\iota) - \frac{\hat{\Lambda}^2}{2\check{\mu}^2\mathcal{N}}\sum_{\iota=1}^N \pi_\iota \sigma_1^2(\iota) - \frac{1}{2\mathcal{N}}\sum_{\iota=1}^N \pi_\iota \frac{\sigma_2^2(\iota)}{\omega^2(\iota)}, \tag{9}$$

$$\mathcal{L} = \left(\frac{\check{\beta}}{\hat{\mu}} + \hat{k}\right)\left(\hat{\mu} + \hat{\varepsilon} + \hat{\gamma} + \frac{\hat{\alpha}}{\check{\omega}}\right), \tag{10}$$

where $\mathcal{N}$ is given by (7). It can be seen that $\mathcal{R}_1^s$ is an approximation of the basic reproduction number $\mathcal{R}_0^s$ defined by (6).

Theorem 3.1. *If $\mathcal{R}_1^s > 1$, then for any initial value $(S_0, I_0, R_0, \vartheta(0)) \in \mathcal{G} \times \mathcal{S}$, the solution $(S(t), I(t), R(t))$ of system* (4) *has the following properties*:

$$(i) \quad \liminf_{t\to\infty} \frac{1}{t}\int_0^t S(\tau)\mathrm{d}\tau \geq \frac{\check{\mu}\sum_{\iota=1}^N \pi_\iota \Lambda(\iota)}{\hat{\beta}\hat{\Lambda} + \hat{\mu}\check{\mu}}, \quad a.s.,$$

$$(ii) \quad \liminf_{t\to\infty} \frac{1}{t}\int_0^t I(\tau)\mathrm{d}\tau \geq \frac{\mathcal{N}}{\mathcal{L}}(\mathcal{R}_1^s - 1), \quad a.s.,$$

$$(iii) \quad \liminf_{t\to\infty} \frac{1}{t}\int_0^t R(\tau)\mathrm{d}\tau \geq \frac{\mathcal{N}}{\hat{\mu}\mathcal{L}}\left(\frac{\check{\alpha}\check{\mu}}{\hat{\omega}\check{\mu} + \hat{\Lambda}} + \check{\gamma}\right)(\mathcal{R}_1^s - 1), \quad a.s.$$

Proof. Let $(S_0, I_0, R_0, \vartheta(0)) \in \mathcal{G} \times \mathcal{S}$. In view of Theorem 2.1, the solution of system (4) remains in $\mathcal{G}$.

(i) From the first equation of system (4) and the fact that $-I(t) \geq -\frac{\hat{\Lambda}}{\check{\mu}}$, we obtain

$$\begin{aligned}
\mathrm{d}S(t) &= \left(\Lambda(\vartheta(t)) - \frac{\beta(\vartheta(t))I(t)S(t)}{1 + k(\vartheta(t))I(t)} - \mu(\vartheta(t))S(t)\right)\mathrm{d}t - \frac{\sigma_1(\vartheta(t))I(t)S(t)}{1 + k(\vartheta(t))I(t)}\mathrm{d}B_1(t) \\
&\geq \left(\Lambda(\vartheta(t)) - \frac{\beta(\vartheta(t))\hat{\Lambda}}{\check{\mu}}S(t) - \mu(\vartheta(t))S(t)\right)\mathrm{d}t - \frac{\sigma_1(\vartheta(t))I(t)S(t)}{1 + k(\vartheta(t))I(t)}\mathrm{d}B_1(t) \\
&\geq \left(\Lambda(\vartheta(t)) - \left(\frac{\hat{\beta}\hat{\Lambda}}{\check{\mu}} + \hat{\mu}\right)S(t)\right)\mathrm{d}t - \frac{\sigma_1(\vartheta(t))I(t)S(t)}{1 + k(\vartheta(t))I(t)}\mathrm{d}B_1(t).
\end{aligned}$$

Integrating the previous inequality from 0 to t and dividing both sides by t, we obtain

$$\frac{S(t)-S_0}{t} \geq \frac{1}{t}\int_0^t \Lambda(\vartheta(\tau))\mathrm{d}\tau - \left(\frac{\hat{\beta}\hat{\Lambda}}{\check{\mu}} + \hat{\mu}\right)\frac{1}{t}\int_0^t S(\tau)\mathrm{d}\tau - \frac{1}{t}\int_0^t \frac{\sigma_1(\vartheta(\tau))I(\tau)S(\tau)}{1+k(\vartheta(\tau))I(\tau)}\mathrm{d}B_1(\tau),$$

and hence,

$$\left(\frac{\hat{\beta}\hat{\Lambda}}{\check{\mu}} + \hat{\mu}\right)\frac{1}{t}\int_0^t S(\tau)\mathrm{d}\tau \geq \frac{1}{t}\int_0^t \Lambda(\vartheta(\tau))\mathrm{d}\tau - \frac{S(t)-S_0}{t} - \frac{\varsigma_0(t)}{t}, \tag{11}$$

where $\varsigma_0(t) = \int_0^t \frac{\sigma_1(\vartheta(\tau))I(\tau)S(\tau)}{1+k(\vartheta(\tau))I(\tau)}\mathrm{d}B_1(\tau)$ is the continuous local martingale such that $\varsigma_0(0) = 0$. Furthermore,

$$\limsup_{t\to\infty}\frac{\langle\varsigma_0,\varsigma_0\rangle}{t} \leq \frac{\hat{\sigma}_1^2\hat{\Lambda}^2}{\check{k}^2\check{\mu}^2} < \infty.$$

Thus, by the strong law of large numbers for local martingales, we obtain

$$\lim_{t\to\infty}\frac{\varsigma_0(t)}{t} = 0. \quad \text{a.s.}$$

Taking the limit inferior on both sides of (11), and using the fact that $0 \leq S(t) \leq \frac{\hat{\Lambda}}{\check{\mu}}$, as well as ergodic property of $\vartheta(t)$, we obtain

$$\liminf_{t\to\infty}\frac{1}{t}\int_0^t S(\tau)\mathrm{d}\tau \geq \frac{\check{\mu}\sum_{\iota=1}^N \pi_\iota\Lambda(\iota)}{\hat{\beta}\hat{\Lambda}+\hat{\mu}\check{\mu}} > 0, \quad \text{a.s.}$$

(*ii*) Summing up the first and second equation of system (4), we have

$$\mathrm{d}(S(t)+I(t)) \geq \left(\Lambda(\vartheta(t)) - \hat{\mu}S(t) - \left(\hat{\mu}+\hat{\varepsilon}+\hat{\gamma}+\frac{\hat{\alpha}}{\check{\omega}}\right)I(t)\right)\mathrm{d}t - \frac{\sigma_2(\vartheta(t))I(t)}{\omega(\vartheta(t))+I(t)}\mathrm{d}B_2(t).$$

Integration of both sides of the previous inequality from 0 to t and division with t, yields

$$\frac{1}{t}\int_0^t S(\tau)\mathrm{d}\tau \geq \frac{1}{\hat{\mu}t}\int_0^t \Lambda(\vartheta(\tau))\mathrm{d}\tau - \frac{\hat{\mu}+\hat{\varepsilon}+\hat{\gamma}+\frac{\hat{\alpha}}{\check{\omega}}}{\hat{\mu}t}\int_0^t I(\tau)\mathrm{d}\tau + \phi(t) - \frac{1}{t}\int_0^t \frac{\sigma_2(\vartheta(\tau))I(\tau)}{\hat{\mu}(\omega(\vartheta(\tau))+I(\tau))}\mathrm{d}B_2(\tau), \tag{12}$$

where $\phi(t) = -\frac{1}{\hat{\mu}t}(S(t)-S_0+I(t)-I_0)$.

By virtue of the generalized Itô formula and the fact that $(S(t), I(t), R(t)) \in \mathcal{G}$, we have

$$\begin{aligned}\mathrm{d}(\ln I(t) + \hat{k}I(t)) \geq \Bigg(&\check{\beta}S(t) - \left(\mu(\vartheta(t)) + \varepsilon(\vartheta(t)) + \gamma(\vartheta(t)) + \frac{\alpha(\vartheta(t))}{\omega(\vartheta(t))}\right) - \hat{k}\left(\hat{\mu}+\hat{\varepsilon}+\hat{\gamma}+\frac{\hat{\alpha}}{\check{\omega}}\right)I(t) - \frac{\sigma_1^2(\vartheta(t))\hat{\Lambda}^2}{2\check{\mu}^2}\\ &- \frac{\sigma_2^2(\vartheta(t))}{2\omega^2(\vartheta(t))}\Bigg)\mathrm{d}t + \frac{\sigma_1(\vartheta(t))S(t)(1+\hat{k}I(t))}{1+k(\vartheta(t))I(t)}\mathrm{d}B_1(t) - \frac{\sigma_2(\vartheta(t))(1+\hat{k}I(t))}{\omega(\vartheta(t))+I(t)}\mathrm{d}B_2(t).\end{aligned}$$

Using (12), we obtain

$$\begin{aligned}&\frac{\ln I(t) - \ln I_0}{t} + \hat{k}\frac{I(t)-I_0}{t}\\ &\geq \frac{\check{\beta}}{\hat{\mu}t}\int_0^t \Lambda(\vartheta(\tau))\mathrm{d}\tau - \frac{1}{t}\int_0^t\left(\mu(\vartheta(\tau)) + \varepsilon(\vartheta(\tau)) + \gamma(\vartheta(\tau)) + \frac{\alpha(\vartheta(\tau))}{\omega(\vartheta(\tau))}\right)\mathrm{d}\tau\\ &\quad - \frac{\hat{\Lambda}^2}{2\check{\mu}^2 t}\int_0^t \sigma_1^2(\vartheta(\tau))\mathrm{d}\tau - \frac{1}{t}\int_0^t \frac{\sigma_2^2(\vartheta(\tau))}{2\omega^2(\vartheta(\tau))}\mathrm{d}\tau + \check{\beta}\phi(t)\\ &\quad - \left(\frac{\check{\beta}}{\hat{\mu}} + \hat{k}\right)\left(\hat{\mu}+\hat{\varepsilon}+\hat{\gamma}+\frac{\hat{\alpha}}{\check{\omega}}\right)\frac{1}{t}\int_0^t I(\tau)\mathrm{d}\tau + \frac{\varsigma_1(t)}{t} - \frac{\varsigma_2(t)}{t} - \frac{\varsigma_3(t)}{t},\end{aligned} \tag{13}$$

where

$$\varsigma_1(t) = \int_0^t \frac{\sigma_1(\vartheta(\tau))S(\tau)(1 + \hat{k}I(\tau))}{1 + k(\vartheta(\tau))I(\tau)} \mathrm{d}B_1(\tau),$$
$$\varsigma_2(t) = \int_0^t \frac{\check{\beta}\sigma_2(\vartheta(\tau))I(\tau)}{\hat{\mu}(\omega(\vartheta(\tau)) + I(\tau))} \mathrm{d}B_2(\tau),$$
$$\varsigma_3(t) = \int_0^t \frac{\sigma_2(\vartheta(\tau))(1 + \hat{k}I(\tau))}{\omega(\vartheta(\tau)) + I(\tau)} \mathrm{d}B_2(\tau)$$

are the continuous local martingales that satisfy $\varsigma_1(0) = \varsigma_2(0) = \varsigma_3(0) = 0$. Furthermore,

$$\limsup_{t\to\infty} \frac{\langle \varsigma_1, \varsigma_1 \rangle}{t} \le \frac{\hat{\sigma}_1^2 \hat{\Lambda}^2}{\check{\mu}^2} \left(1 + \hat{k}\frac{\hat{\Lambda}}{\check{\mu}}\right)^2 < \infty,$$
$$\limsup_{t\to\infty} \frac{\langle \varsigma_2, \varsigma_2 \rangle}{t} \le \frac{\check{\beta}^2 \hat{\sigma}_2^2}{\hat{\mu}^2} < \infty,$$
$$\limsup_{t\to\infty} \frac{\langle \varsigma_3, \varsigma_3 \rangle}{t} \le \frac{\hat{\sigma}_2^2}{\check{\omega}^2} \left(1 + \hat{k}\frac{\hat{\Lambda}}{\check{\mu}}\right)^2 < \infty.$$

Thus, in view of the strong law of large numbers for local martingales, we have

$$\lim_{t\to\infty} \frac{\varsigma_1(t)}{t} = \lim_{t\to\infty} \frac{\varsigma_2(t)}{t} = \lim_{t\to\infty} \frac{\varsigma_3(t)}{t} = 0, \quad \text{a.s.}$$

According to Theorem 2.1, we have $-\infty < \ln I \le \ln \frac{\hat{\Lambda}}{\check{\mu}}$ and $\lim_{t\to\infty} \phi(t) = 0$ a.s. Taking the limit inferior of both sides of (13) and using the fact that $\vartheta(t)$ has the ergodic property, we conclude

$$\liminf_{t\to\infty} \frac{1}{t} \int_0^t I(\tau)\mathrm{d}\tau \ge \frac{\mathcal{N}}{\mathcal{L}}(\mathcal{R}_1^s - 1) > 0, \quad \text{a.s.}$$

(*iii*) From the last equation of system (4), bearing in mind that $I(t) \le \frac{\hat{\Lambda}}{\check{\mu}}$, we obtain

$$\mathrm{d}R(t) \ge \left(\left(\frac{\check{\alpha}\check{\mu}}{\hat{\omega}\check{\mu} + \hat{\Lambda}} + \check{\gamma}\right) I(t) - \hat{\mu}R(t)\right)\mathrm{d}t + \frac{\sigma_2(\vartheta(t))I(t)}{\omega(\vartheta(t)) + I(t)} \mathrm{d}B_2(t).$$

If we integrate the aforementioned inequality from 0 to t and divide both sides by t, we conclude that

$$\frac{1}{t}\int_0^t R(\tau)\mathrm{d}\tau \ge \frac{1}{\hat{\mu}}\left(\left(\frac{\check{\alpha}\check{\mu}}{\hat{\omega}\check{\mu} + \hat{\Lambda}} + \check{\gamma}\right)\frac{1}{t}\int_0^t I(\tau)\mathrm{d}\tau - \frac{R(t) - R_0}{t} + \frac{\varsigma_4}{t}\right), \tag{14}$$

where $\varsigma_4(t) = \int_0^t \frac{\sigma_2(\vartheta(\tau))I(\tau)}{\omega(\vartheta(\tau)) + I(\tau)} \mathrm{d}B_2(\tau)$ is the continuous local martingale and $\varsigma_4(0) = 0$. By the same arguments as in the proof of (*ii*), we obtain that

$$\lim_{t\to\infty} \frac{\varsigma_4(t)}{t} = 0, \quad \text{a.s.}$$

Taking the limit inferior on both sides of (14), using (*ii*), as well as $0 \le R(t) \le \frac{\hat{\Lambda}}{\check{\mu}}$, we obtain

$$\liminf_{t\to\infty} \frac{1}{t}\int_0^t R(\tau)\mathrm{d}\tau \ge \frac{\mathcal{N}}{\hat{\mu}\mathcal{L}}\left(\frac{\check{\alpha}\check{\mu}}{\hat{\omega}\check{\mu} + \hat{\Lambda}} + \check{\gamma}\right)(\mathcal{R}_1^s - 1) > 0, \quad \text{a.s.}$$

4 Extinction of the disease

In this section, we will focus on obtaining the conditions under which the disease dies out in the population. Determining these conditions is important because they provide a way to control the epidemic. For that purpose, we define

$$\mathcal{R}_2^s = \frac{\hat{\Lambda}}{\mathcal{N}\check{\mu}}\sum_{\iota=1}^{N}\pi_\iota\beta(\iota) - \frac{\hat{\Lambda}^2}{2\mathcal{N}\check{\mu}^2}\sum_{\iota=1}^{N}\pi_\iota\sigma_1^2(\iota) - \frac{1}{2\mathcal{N}}\sum_{\iota=1}^{N}\pi_\iota\frac{\sigma_2^2(\iota)}{\omega^2(\iota)}, \tag{15}$$

$$\mathcal{T} = \frac{1}{\mathcal{N}}\sum_{\iota=1}^{N}\pi_\iota\frac{2\alpha(\iota)}{\omega(\iota)}, \tag{16}$$

$$\mathcal{J} = \sum_{\iota=1}^{N}\pi_\iota\left(\frac{\beta^2(\iota)}{2\sigma_1^2(\iota)} + \frac{\alpha^2(\iota)}{2\sigma_2^2(\iota)} - (\mu(\iota)+\varepsilon(\iota)+\gamma(\iota))\right), \tag{17}$$

where $\mathcal{N}$ is given by (7). Moreover, $\mathcal{R}_2^s$ is an approximation of the basic reproduction number $\mathcal{R}_0^s$ defined by (6).

Theorem 4.1. *If the one of following conditions hold*
Case (i)

$$\hat{\sigma}_1^2 \le \frac{\check{\mu}\check{\beta}}{\hat{\Lambda}}, \tag{18}$$

$$\hat{\sigma}_2{}^2 \le \check{\alpha}\check{\omega}, \tag{19}$$

$$\mathcal{R}_2^s + \mathcal{T} < 1, \tag{20}$$

or
Case (ii)

$$\mathcal{J} < 0, \tag{21}$$

then the disease will die out exponentially with probability 1, i.e.

$$\lim_{t\to\infty} I(t) = 0, \quad a.s.$$

Proof. With the same reasoning as in the previous proofs, we suppose that $(S_0, I_0, R_0, \vartheta(0)) \in \mathcal{G}\times\mathcal{S}$. Applying the generalized Itô formula to the second equation of (4), we obtain

$$\mathrm{d}\ln I(t) = LV\mathrm{d}t + \frac{\sigma_1(\vartheta(t))S(t)}{1+k(\vartheta(t))I(t)}\mathrm{d}B_1(t) - \frac{\sigma_2(\vartheta(t))}{\omega(\vartheta(t))+I(t)}\mathrm{d}B_2(t),$$

where

$$\begin{aligned} LV = {} & \frac{\beta(\vartheta(t))S(t)}{1+k(\vartheta(t))I(t)} - (\mu(\vartheta(t))+\varepsilon(\vartheta(t))+\gamma(\vartheta(t))) - \frac{\alpha(\vartheta(t))}{\omega(\vartheta(t))+I(t)} \\ & - \frac{1}{2}\left[\left(\frac{\sigma_1(\vartheta(t))S(t)}{1+k(\vartheta(t))I(t)}\right)^2 + \left(\frac{\sigma_2(\vartheta(t))}{\omega(\vartheta(t))+I(t)}\right)^2\right]. \end{aligned} \tag{22}$$

Case (i): We can rewrite LV defined by (22) as

$$\begin{aligned} LV = {} & \frac{\beta(\vartheta(t))S(t)}{1+k(\vartheta(t))I(t)} - \left(\mu(\vartheta(t))+\varepsilon(\vartheta(t))+\gamma(\vartheta(t))+\frac{\alpha(\vartheta(t))}{\omega(\vartheta(t))}\right) - \frac{2\alpha(\vartheta(t))}{\omega(\vartheta(t))+I(t)} \\ & + \frac{\alpha(\vartheta(t))}{\omega(\vartheta(t))+I(t)} + \frac{\alpha(\vartheta(t))}{\omega(\vartheta(t))} - \frac{1}{2}\left[\left(\frac{\sigma_1(\vartheta(t))S(t)}{1+k(\vartheta(t))I(t)}\right)^2 + \left(\frac{\sigma_2(\vartheta(t))}{\omega(\vartheta(t))+I(t)}\right)^2\right] \\ \le {} & \Phi_1(x) + \Phi_2(y), \end{aligned}$$

where

$$\Phi_1(x) = -\frac{\sigma_1^2(\vartheta(t))}{2}x^2 + \beta(\vartheta(t))x - \left(\mu(\vartheta(t)) + \varepsilon(\vartheta(t)) + \gamma(\vartheta(t)) + \frac{\alpha(\vartheta(t))}{\omega(\vartheta(t))}\right),$$

for $x = \frac{S(t)}{1+k(\vartheta(t))I(t)}$, and

$$\Phi_2(y) = -\frac{\sigma_2^2(\vartheta(t))}{2\omega^2(\vartheta(t))}y^2 + \frac{\alpha(\vartheta(t))}{\omega(\vartheta(t))}y + \frac{\alpha(\vartheta(t))}{\omega(\vartheta(t))},$$

for $y = \frac{1}{1+\frac{I(t)}{\omega(\vartheta(t))}}$. From conditions (18) and (19) we have that the functions $\Phi_1(x)$ and $\Phi_2(y)$ are monotone increasing for all $x \le \frac{\hat{\Lambda}}{\check{\mu}}$ and $y \le 1$, respectively, and, thus, we have $\Phi_1(x) \le \Phi_1(S(t)) \le \Phi_1\left(\frac{\hat{\Lambda}}{\check{\mu}}\right)$ and $\Phi_2(y) \le \Phi_2(1)$. Hence,

$$LV \le \frac{\hat{\Lambda}\beta(\vartheta(t))}{\check{\mu}} - \left(\mu(\vartheta(t)) + \varepsilon(\vartheta(t)) + \gamma(\vartheta(t)) + \frac{\alpha(\vartheta(t))}{\omega(\vartheta(t))}\right) - \frac{\hat{\Lambda}^2\sigma_1^2(\vartheta(t))}{2\check{\mu}^2} - \frac{\sigma_2^2(\vartheta(t))}{2\omega^2(\vartheta(t))} + \frac{2\alpha(\vartheta(t))}{\omega(\vartheta(t))} \coloneqq C_1(\vartheta(t)).$$

Integrating $\mathrm{d}\ln I(t)$ from 0 to t and dividing both sides by t, yield

$$\frac{\ln I(t) - \ln I_0}{t} \le \frac{1}{t}\int_0^t C_1(\vartheta(\tau))\mathrm{d}\tau + \frac{\varsigma_5(t)}{t} - \frac{\varsigma_6(t)}{t}, \tag{23}$$

where $\varsigma_5(t) = \int_0^t \frac{\sigma_1(\vartheta(\tau))S(\tau)}{1+k(\vartheta(\tau))I(\tau)}\mathrm{d}B_1(\tau)$, and $\varsigma_6(t) = \int_0^t \frac{\sigma_2(\vartheta(\tau))}{\omega(\vartheta(\tau))+I(\tau)}\mathrm{d}B_2(\tau)$ are the continuous local martingales and $\varsigma_5(0) = \varsigma_6(0) = 0$. By the same arguments as in the proof of Theorem 3.1, we obtain that

$$\lim_{t\to\infty}\frac{\varsigma_5(t)}{t} = \lim_{t\to\infty}\frac{\varsigma_6(t)}{t} = 0, \quad \text{a.s.}$$

As $\vartheta(t)$ has the ergodic property, we conclude

$$\limsup_{t\to\infty}\frac{1}{t}\int_0^t C_1(\vartheta(\tau))\mathrm{d}\tau = \sum_{\iota=1}^N \pi_\iota C_1(\iota).$$

Finally, taking the limit superior on both sides of (23) and using condition (20) and definition (7) of constant $\mathcal{N}$, we arrive at

$$\limsup_{t\to\infty}\frac{\ln I(t)}{t} \le \sum_{\iota=1}^N \pi_\iota C_1(\iota) = \mathcal{N}(\mathcal{R}_2^s + \mathcal{T} - 1) < 0, \quad \text{a.s.}$$

Case (ii): Bearing in mind (22), we obtain

$$\begin{aligned} LV = &-\frac{\sigma_1^2(\vartheta(t))}{2}\left(\frac{S(t)}{1+k(\vartheta(t))I(t)} - \frac{\beta(\vartheta(t))}{\sigma_1^2(\vartheta(t))}\right)^2 + \frac{\beta^2(\vartheta(t))}{2\sigma_1^2(\vartheta(t))} \\ &- \frac{\sigma_2^2(\vartheta(t))}{2}\left(\frac{1}{\omega(\vartheta(t))+I(t)} + \frac{\alpha(\vartheta(t))}{\sigma_2^2(\vartheta(t))}\right)^2 + \frac{\alpha^2(\vartheta(t))}{2\sigma_2^2(\vartheta(t))} - (\mu(\vartheta(t)) + \varepsilon(\vartheta(t)) + \gamma(\vartheta(t))) \\ \le &\frac{\beta^2(\vartheta(t))}{2\sigma_1^2(\vartheta(t))} + \frac{\alpha^2(\vartheta(t))}{2\sigma_2^2(\vartheta(t))} - (\mu(\vartheta(t)) + \varepsilon(\vartheta(t)) + \gamma(\vartheta(t))) \coloneqq C_2(\vartheta(t)). \end{aligned}$$

Based on the ergodic property of $\vartheta(t)$, we obtain

$$\limsup_{t\to\infty}\frac{1}{t}\int_0^t C_2(\vartheta(\tau))\mathrm{d}\tau = \sum_{\iota=1}^N \pi_\iota C_2(\iota).$$

By the same arguments as in the proof of **Case (i)**, using condition (21), we have

$$\limsup_{t\to\infty}\frac{\ln I(t)}{t} \le \sum_{\iota=1}^{N}\pi_\iota C_2(\iota) = \mathcal{J} < 0, \quad \text{a.s.}$$

Cases (i) and **(ii)** imply that $\lim_{t\to\infty} I(t) = 0$ a.s.

Remark 1. The previous theorem tells us that the disease goes extinct if white noises are not large and condition (20) holds, or if white noises are large enough such that condition (21) is satisfied.

Remark 2. Lately, the catastrophic earthquakes in Turkey, Syria, and Japan, as well as the civil wars in Ukraine and Gaza, have a significant impact on the spread of the diseases. We may consider them as noises with high intensities, and that is the reason why condition (21) is particularly important, since it gives us a way to control the epidemic.

Remark 3. If the intensities of the white noises are small enough and condition $\mathcal{R}_2^s + \mathcal{T} < 1$ is satisfied, from Theorem 4.1, we may conclude that the disease will die out. Bearing in mind definitions of constants $\mathcal{R}_1^s$ and $\mathcal{R}_2^s$, it is obvious that $\mathcal{R}_1^s < \mathcal{R}_2^s$, i.e. $\mathcal{R}_1^s < 1$. On the other hand, if $\mathcal{R}_1^s > 1$, the disease is persistent in mean. Then, we have that $\mathcal{R}_2^s + \mathcal{T} > 1$. Thus, we can regard this fact as a threshold in the behaviour of the disease.

5 Numerical simulation

In order to confirm theoretical results obtained throughout this study, we present numerical simulations of model (4) with real-life data. For that purpose, we use the Milstein higher-order method mentioned in [27]. We assume that driving process $\{\vartheta(t), t \ge 0\}$ is a right-continuous Markov chain taking values in $\mathcal{S} = \{1, 2\}$. For each environmental state $\iota \in \mathcal{S}$, we have the discretization equation of system:

$$\begin{aligned}
S_{k+1} &= S_k + \left(\Lambda(\iota) - \frac{\beta(\iota)I_kS_k}{1+k(\iota)I_k} - \mu(\iota)S_k\right)\Delta t - \frac{\sigma_1(\iota)I_kS_k}{1+k(\iota)I_k}\sqrt{\Delta t}\,\eta_{1,k} - \frac{\sigma_1^2(\iota)}{2}\frac{S_k}{1+k(\iota)I_k}(\eta_{1,k}^2 - 1)\Delta t,\\
I_{k+1} &= I_k + \left(\frac{\beta(\iota)I_kS_k}{1+k(\iota)I_k} - (\mu(\iota)+\varepsilon(\iota)+\gamma(\iota))I_k - \frac{\alpha(\iota)I_k}{\omega(\iota)+I_k}\right)\Delta t + \frac{\sigma_1(\iota)I_kS_k}{1+k(\iota)I_k}\sqrt{\Delta t}\,\eta_{1,k} + \frac{\sigma_1^2(\iota)}{2}\frac{S_k}{1+k(\iota)I_k}(\eta_{1,k}^2 - 1)\Delta t\\
&\quad - \frac{\sigma_2(\iota)I_k}{\omega(\iota)+I_k}\sqrt{\Delta t}\,\eta_{2,k} - \frac{\sigma_2^2(\iota)}{2}\frac{I_k}{\omega(\iota)+I_k}(\eta_{2,k}^2 - 1)\Delta t,\\
R_{k+1} &= R_k + \left(\gamma(\iota)I_k + \frac{\alpha(\iota)I_k}{\omega(\iota)+I_k} - \mu(\iota)R_k\right)\Delta t + \frac{\sigma_2(\iota)I_k}{\omega(\iota)+I_k}\sqrt{\Delta t}\,\eta_{2,k} + \frac{\sigma_2^2(\iota)}{2}\frac{I_k}{\omega(\iota)+I_k}(\eta_{2,k}^2 - 1)\Delta t,
\end{aligned}$$

where $\eta_{1,k}$, $\eta_{2,k}$, $k = 1,\dots,n$, are the independent Gaussian random variables $N(0,1)$ and $\Delta t > 0$ is the time increment.

5.1 Example 1: Ebola outbreak in Sierra Leone, 2014–2016

Ebola virus disease (EVD) is a rare but severe, often fatal illness in humans. This deadly disease occurs primarily as a result of the transmission of the deadly Ebola virus from wild animals, especially bats, to the human population. Further spread of EVD includes human-to-human transmission. The average EVD case fatality rate is around 50%. Case fatality rates have varied from 25 to 90% in past outbreaks. Symptoms of EVD can be sudden and include fever, fatigue, muscle pain, headache, and sore throat.

The 2014–2016 outbreak in West Africa was the largest Ebola outbreak since the virus was first discovered in 1976. The outbreak started in Guinea and then moved across land borders to Sierra Leone and Liberia. In this period, there was no vaccine.

In the literature (see [28,29], for example), it can be found that climatic and seasonal factors affect the spread of the Ebola virus. The highest intensity of Ebola virus transmission is in the rainy season, after the long dry season which is the breeding season for fruit bats, reservoirs of the Ebola virus. In Sierra Leone, there is a rainy season for about 6 months (from April to July, October, and November). For that reason, we set $\mathcal{S} = \{1, 2\}$, where state 1 and state 2 represent the rainy and dry season, respectively, and generator matrix is

$$Q = \begin{bmatrix} -1 & 1 \\ 1 & -1 \end{bmatrix}.$$

Thus, $\pi_1 = \pi_2 = 0.5$.

The values of the parameters of model (4) were obtained from [28,30,31]:

$$\begin{aligned} &\Lambda(1) = \Lambda(2) = 36.023 \quad \text{per} \quad 1000, && \mu(1) = \mu(2) = 0.013355, \\ &\beta(1) = 0.001, \quad \beta(2) = 0.00064, && k(1) = 0.7, \quad k(2) = 0.8, \\ &\varepsilon(1) = 0.28, \quad \varepsilon(2) = 0.69, && \gamma(1) = 0.52, \quad \gamma(2) = 0.15, \\ &\alpha(1) = 0.005, \quad \alpha(2) = 0.006, && \omega(1) = 350, \quad \omega(2) = 400. \end{aligned} \tag{24}$$

We choose intensities of the noises

$$\begin{aligned} &\sigma_1^2(1) = 0.00003, \quad \sigma_1^2(2) = 0.00001, \\ &\sigma_2^2(1) = 0.001, \quad \sigma_2^2(2) = 0.002, \end{aligned} \tag{25}$$

and initial condition

$$(S_0,\ I_0,\ R_0,\ \vartheta(0)) = (1000,\ 10,\ 2,\ 1). \tag{26}$$

For these parameter values, we obtain that the condition (21) of Theorem 4.1 is satisfied and extinction of the disease occurs (Figures 1–3).

In Figure 1, we can see that the red trajectory approaches zero in approximately 2 years, which means that the epidemic will disappear in 2 years, and this scenario really occurred during the Ebola outbreak in Sierra Leone. On the other hand, the black trajectory indicates that the disease will persist, which means that white noise has a greater contribution in extinction compered to coloured noise. If we compute basic reproduction numbers for the first and the second states for model (2) from definition (5), we obtain $\mathcal{R}_0(1) = 3.216 > 1$ and $\mathcal{R}_0(2) = 1.896 > 1$. Hence, it is expected for disease-free equilibrium of deterministic model (2) to be unstable, on the basis of Theorem 3.1 from [1]. This is also confirmed by the simulations in Figures 2 and 3. Namely, in Figure 2 (right), we can see that both blue and black trajectories for $S(t)$ approach the total number $\frac{\hat{\Lambda}}{\hat{\mu}} = 2697.34$. Furthermore, $R(t)$ approaches zero if it is exposed to white noise (green line in Figure 3 (right))

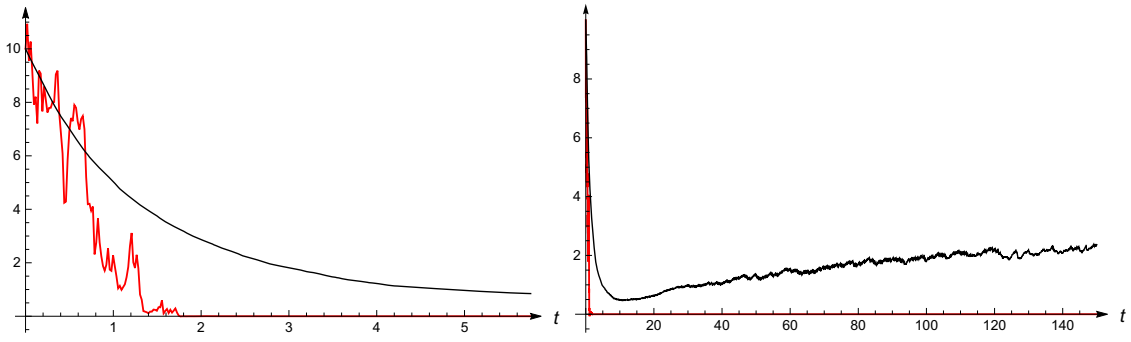

Figure 1: Trajectories of infected individuals $I(t)$ for period of 5 years (left) and 150 years (right) of model (4) with model parameters (24), initial condition (26), and intensities of white noise (25) (red line) and $\sigma_1^2(1) = \sigma_1^2(2) = \sigma_2^2(1) = \sigma_2^2(2) = 0$ (black line).

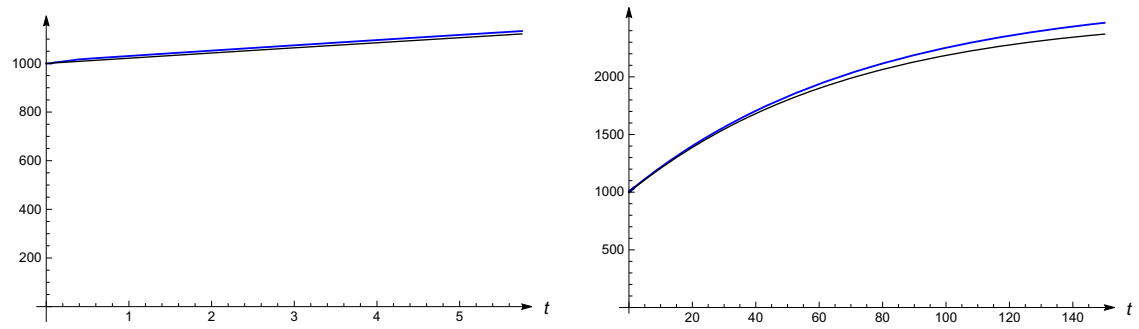

Figure 2: Trajectories of susceptible individuals $S(t)$ for period of 5 years (left) and 150 years (right) of model (4) with model parameters (24), initial condition (26), and intensities of white noise (25) (blue line) and $\sigma_1^2(1) = \sigma_1^2(2) = \sigma_2^2(1) = \sigma_2^2(2) = 0$ (black line).

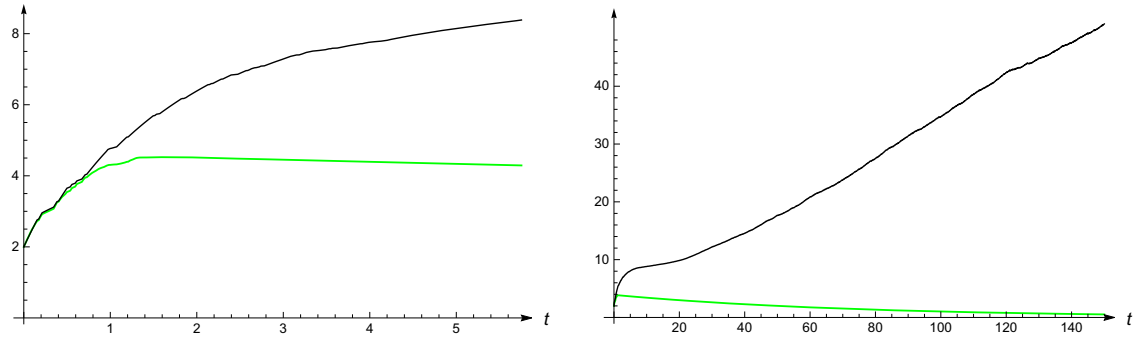

Figure 3: Trajectories of recovered individuals $R(t)$ for period of 5 years (left) and 150 years (right) of model (4) with model parameters (24), initial condition (26), and intensities of white noise (25) (green line) and $\sigma_1^2(1) = \sigma_1^2(2) = \sigma_2^2(1) = \sigma_2^2(2) = 0$ (black line).

for a sufficiently long time, more precisely until all those in group R with permanent immunity die. But, in case where intensities of the white noise are equal to zero, the disease persists and we have an increasing number of recovered individuals.

5.2 Example 2: COVID-19 pandemic in Pakistan

The COVID-19 pandemic started in December 2019, when the first case of a new respiratory illness was reported in Wuhan, China. The virus responsible for the illness was identified as a novel coronavirus, which was later named severe acute respiratory syndrome coronavirus 2.

Pakistan had been hit hard by the COVID-19 pandemic, with thousands of new cases and hundreds of deaths being reported each day. The first case of COVID-19 in Pakistan was reported in February 2020, and since then, the country has struggled to contain the spread of the virus. One of the biggest challenges that Pakistan was facing during the pandemic has been its healthcare system. The country has a limited number of hospital beds and medical staff, and many hospitals have been overwhelmed with COVID-19 patients. In addition, there have been shortages of essential medical supplies, such as oxygen and personal protective equipment.

For this simulation, we used data for Pakistan for the months of April, May, and June 2021, because on the fact that our model does not include vaccination, and in that period, the vaccine was not available to everyone. More precisely, the first doses of the vaccine arrived to Pakistan in May 2021 [32]. The situation in Pakistan during April, May, and June 2021 was challenging, with the country struggling to stop the spread of the virus amid a surge in cases and deaths. The country had initially managed to control the spread of the virus through

strict lockdowns and other measures, but a new wave of infections had begun in March 2021, and by April, the situation had become critical.

In April, Pakistan was reporting thousands of new cases and hundreds of deaths each day, with hospitals struggling to cope with the influx of patients. One of the factors contributing to the surge in cases was the emergence of new variants of the virus. In that period, two variants of the coronavirus were dominant. The Alpha variant, also known as B.1.1.7, was first identified in the United Kingdom in late 2020. It is believed to be more infectious than the original strain of the virus, and has been associated with increased transmissibility and a higher risk of hospitalization and death. The second is the Beta variant, also known as B.1.351, which was first identified in South Africa in late 2020. Like the Alpha variant, it is believed to be more infectious and potentially more resistant to vaccines than the original strain of the virus. The Alpha variant was predominant at 82.5 and 40.3% of the cases in April and May 2021, respectively. The Beta variant increased in May (29%) and June (42%) and then reduced to 6% by July [33]. For that reason, state 1 denotes the Alpha variant and state 2 the Beta variant. We set $\mathcal{S} = \{1, 2\}$ and generator matrix

$$Q = \begin{bmatrix} -2 & 2 \\ 3 & -3 \end{bmatrix}.$$

We have $\pi_1 = 0.6$ and $\pi_2 = 0.4$.

From [34], we obtain values of the parameters of model (4):

$$\begin{aligned} &\Lambda(1) = \Lambda(2) = 27.034 \quad \text{per} \quad 1000, && \mu(1) = \mu(2) = 0.006835, \\ &\beta(1) = 0.0018, \quad \beta(2) = 0.00059, && k(1) = k(2) = 0.62, \\ &\varepsilon(1) = 0.0238, \quad \varepsilon(2) = 0.0242, && \gamma(1) = 0.92, \quad \gamma(2) = 0.9, \\ &\alpha(1) = \alpha(2) = 0.001, && \omega(1) = \omega(2) = 700. \end{aligned} \tag{27}$$

We choose intensities of the noises

$$\begin{aligned} &\sigma_1^2(1) = 0.00000006, \quad \sigma_1^2(2) = 0.0000001, \\ &\sigma_2^2(1) = 0.06, \qquad\qquad \sigma_2^2(2) = 0.03, \end{aligned} \tag{28}$$

and initial condition

$$(S_0,\ I_0,\ R_0,\ \vartheta(0)) = (1000, 5,\ 10,\ 1). \tag{29}$$

If we compute $\mathcal{R}_1^s = 1.84464 > 1$, from Theorem 3.1, we expect the solution of model (4) to be persistent in mean, which may be seen in Figures 4 and 5. Moreover, if we check the current data for Pakistan on [34], about 3 years after the initial moment, we can note that the cases of COVID-19 are still being recorded and that number is at a low level. This situation is represented in Figure 4.

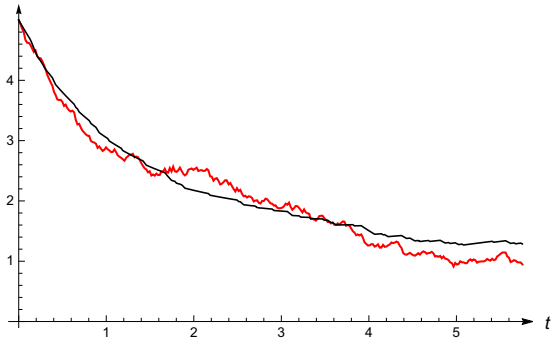

Figure 4: Trajectories of infected individuals $I(t)$ for period of 5 years of model (4) with model parameters (27), initial condition (29), and intensities of white noise (28) (red line) and $\sigma_1^2(1) = \sigma_1^2(2) = \sigma_2^2(1) = \sigma_2^2(2) = 0$ (black line).

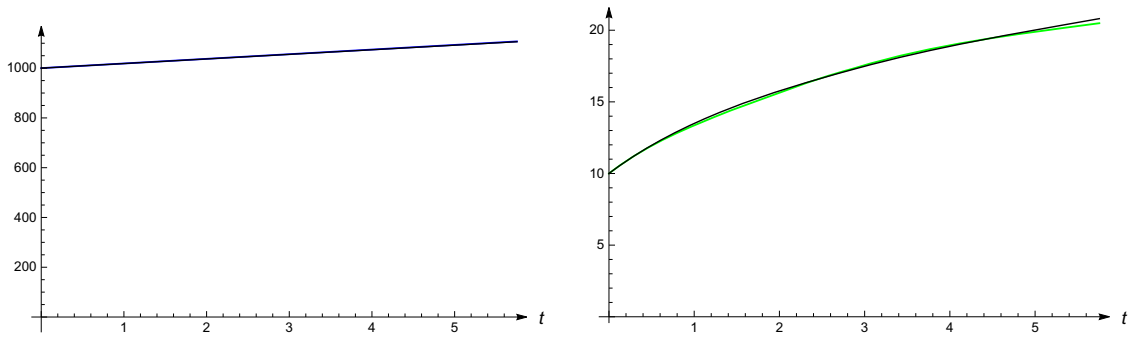

Figure 5: Trajectories of susceptible individuals $S(t)$ (left) and recovered individuals $R(t)$ (right) for period of 5 years of model (4) with model parameters (27), initial condition (29), and intensities of white noise (28) (blue line and green line) and $\sigma_1^2(1) = \sigma_1^2(2) = \sigma_2^2(1) = \sigma_2^2(2) = 0$ (black line).

6 Conclusion

In this article, we consider a stochastic SIR epidemic model with saturated incidence function, as well as treatment function. Moreover, in addition to the white noise, we introduce telegraphic noise. For example, external factors such as seasonal changes, or the presence of different variants of the virus, may affect the spread of the disease. Hence, it is justified to assume that the disease spread can switch between two or more regimes.

For model (4), we proved

- the existence and uniqueness of the positive solution,
- the conditions under which the disease persists in the population and these under which the disease dies out,
- connection between critical values for the survival and extinction of diseases, which can be viewed as a threshold value,
- the conditions for disease extinction for small and large noise.

In order to verify our theoretical results, we performed numerical simulations with real-life data. Based on the simulations, we may conclude that model (4) closely approaches reality, and predicts well the further course of the disease. This gives us the right to claim that model (4) can be a good basis for further analysis of the diseases to which the recovered individuals acquire permanent immunity. The model can be further improved by introducing the Lévy process to describe the phenomena that cause a big jump to occur occasionally and describe sudden and unexpected external phenomena, as it was done in [35–38]. Our aim is to describe the strong fluctuations induced by certain sudden environmental catastrophes, such as earthquakes, floods, and droughts (we already mentioned severe earthquakes in Turkey, Syria, and Japan, which happened lately) since the impact of this unexpected disasters has been extremely devastating, especially when it has occurred simultaneously with the ongoing epidemics.

Acknowledgement: The author extends her appreciations to the editor and anonymous referees for their very helpful comments and suggestions, which greatly improved this article.

Funding information: This research was financially supported by the Ministry of Science, Technological Development and Innovation of the Republic of Serbia (Contract No. 451-03-137/2025-03/200109).

Author contributions: The author confirms the sole responsibility for the conception of the study, presented results, and prepared the manuscript.

Conflict of interest: The author has no conflicts of interest to declare that are relevant to the content of this article.

Data availability statement: All data generated or analysed during this study are included in this published article.

References

[1] L. Zhou and M. Fan, *Dynamics of an SIR epidemic model with limited medical resources revisted*, Nonlinear Anal. Real World Appl. **13** (2012), no. 1, 312–324, DOI: https://doi.org/10.1016/j.nonrwa.2011.07.036.

[2] R. Alqahtani, *Mathematical model of SIR epidemic system (COVID-19) with fractional derivative: stability and numerical analysis*, Adv. Differ. Equ. **2021** (2021), 2, DOI: https://doi.org/10.1186/s13662-020-03192-w.

[3] M. De la Sen and A. Ibeas, *On an SIR epidemic model for the COVID-19 pandemic and the logistic equation*, Discrete Dyn. Nature Soc. **2020** (2020), 1382870, DOI: https://doi.org/10.1155/2020/1382870.

[4] W. Kermack and A. McKendrick, *Contributions to the mathematical theory of epidemics I*, Bull. Math. Biol. **53** (1991), no. 1–2, 33–55, DOI: https://doi.org/10.1007/BF02464423.

[5] W. Kermack and A. McKendrick, *Contributions to the mathematical theory of epidemics II. The problem of endemicity 1932*, Bull. Math. Biol. **53** (1991), no. 1–2, 57–87, DOI: https://doi.org/10.1007/BF02464424.

[6] W. Kermack and A. McKendrick, *Contributions to the mathematical theory of epidemics III. Further studies of the problem of endemicity 1933*, Bull. Math. Biol. **53** (1991), no. 1–2, 89–118, DOI: https://doi.org/10.1007/BF02464425.

[7] D. Li, J. Cui, M. Liu, and S. Liu, *The evolutionary dynamics of stochastic epidemic model with nonlinear incidence rate*, Bull. Math. Biol. **77** (2015), 1705–1743, DOI: https://doi.org/10.1007/s11538-015-0101-9.

[8] S. P. Rajasekar, M. Pitchaimani, and Q. Zhu, *Dynamic threshold probe of stochastic SIR model with saturated incidence rate and saturated treatment function*, Phys. A **535** (2019), 122300, DOI: https://doi.org/10.1016/j.physa.2019.122300.

[9] C. Ji, D. Jiang, and N. Shi, *The behaviour of an SIR epidemic model with stochastic perturbation*, Stoch. Anal. Appl. **30** (2012), no. 5, 755–773, DOI: https://doi.org/10.1080/07362994.2012.684319.

[10] C. Jia and D. Jiang, *Threshold behaviour of a stochastic SIR model*, Appl. Math. Model. **38** (2014), no. 21–21, 5067–5079, DOI: https://doi.org/10.1016/j.apm.2014.03.037.

[11] Q. Liu, D. Jiang, T. Hayat, and B. Ahmad, *Stationary distribution and extinction of a stochastic SIRI epidemic model with relapse*, Stoch. Anal. Appl. **36** (2018), no. 1, 138–151, DOI: https://doi.org/10.1080/07362994.2017.1378897.

[12] M. Milunović and M. Krstić, *Long time behaviour of an two diffusion stochastic SIR epidemic model with nonlinear incidence and treatment*, Filomat **36** (2022), no. 8, 2829–2846.

[13] M. N'zi and J. Tano, *Deterministic and stochastic stability of an SIRS epidemic model with a saturated incidence rate*, Random Oper. Stoch. Equ. **25** (2017), no. 1, 11–26, DOI: https://doi.org/10.1515/rose-2017-0002.

[14] M. Krstić, *The effect of stochastic perturbation on a nonlinear delay malaria epidemic model*, Math. Comput. Simulation **82** (2011), 558–569, DOI: https://doi.org/10.1016/j.matcom.2011.09.003.

[15] M. Marković and M. Krstić, *On a stochastic generalized delayed SIR model with vaccination and treatment*, Nonlinearity **36** (2023), no. 12, 7007, DOI: https://doi.org/10.1088/1361-6544/ad08fb.

[16] M. Jovanović and M. Krstić, *Stochastically perturbed vector-borne disease models with direct transmission*, Appl. Math. Model. **36** (2012), no. 11, 5214–5228, DOI: https://doi.org/10.1016/j.apm.2011.11.087.

[17] S. Bonaccorsi and S. Ottaviano, *A stochastic differential equation SIS model on network under Markovian switching*, Stoch. Anal. Appl. **41** (2023), no. 6, 1231–1259, DOI: https://doi.org/10.1080/07362994.2022.2146590.

[18] Z. Cao, X. Liu, X. Wen, L. Liu, and L. Zu, *A regime-switching SIR epidemic model with a ratio-dependent incidence rate and degenerate diffusion*, Sci. Rep. **9** (2019), 10696, DOI: https://doi.org/10.1038/s41598-019-47131-6.

[19] Y. Ding, J. Jiao, Q. Zhang, Y. Zhang, and X. Ren, *Stationary distribution and extinction in a stochastic SIQR epidemic model incorporating media coverage and Markovian switching*, Symmetry **13** (2021), no. 7, 1122, DOI: https://doi.org/10.3390/sym13071122.

[20] X. Gua and J. Luo, *Stationary distribution and extinction of SIR model with nonlinear incident rate under Markovian switching*, Phys. A **505** (2018), 471–481, DOI: https://doi.org/10.1016/j.physa.2018.02.024.

[21] A. El Koufi, A. Bennar, and N. Yousfi, *Dynamics of a stochastic SIRS epidemic model with regime switching and specific functional response*, Discrete Dyn. Nature Soc. **2020** (2020), 5898456, DOI: https://doi.org/10.1155/2020/5898456.

[22] M. Krstić, V. Vujović, and M. Marković, *Stationary distribution and extinction in the stochastic model of human immune system response to COVID-19 virus under regime switching*, Analele. Ştiint. ale Univ. Ovidius Constanta: Seria Matematica **33** (2025), no. 1, 215–237. DOI: https://doi.org/10.2478/auom-2025-0011.

[23] L. Liu, D. Jiang, and T. Hayat, *Dynamics of an SIR epidemic model with varying population sizes and regime switching in a two patch setting*, Phys. A **574** (2021), 125992, DOI: https://doi.org/10.1016/j.physa.2021.125992.

[24] Z. Wang and Q. Zhang, *Positivity-preserving numerical method and relaxed control for stochastic susceptible-infected-vaccinated epidemic model with Markov switching*, J. Comput. Biol. **30** (2023), no. 6, 695–725, DOI: https://doi.org/10.1089/cmb.2022.0388.
[25] W. Wei, W. Xu, and J. Liu, *A regime-switching stochastic SIR epidemic model with a saturated incidence and limited medical resources*, Int. J. Biomath. **16** (2023), no. 7, 2250124, DOI: https://doi.org/10.1142/S1793524522501248.
[26] J. Xu, Y. Wang, and Z. Cao, *Dynamics of a stochastic SIRS epidemic model with standard incidence under regime switching*, Int. J. Biomath. **15** (2022), no. 2, 2150074, DOI: https://doi.org/10.1142/S1793524521500741.
[27] D. J. Higham, *An algorithmic introduction to numerical simulation of stochastic differential equations*, SIAM Rev. **43** (2001), no. 3, 525–546, DOI: http://dx.doi.org/10.1137/S0036144500378302.
[28] R. T. Kamorudeen, K. A. Adedokun, and A. O. Olarinmoye, *Ebola outbreak in West Africa, 2014–2016: Epidemic timeline, differential diagnoses, determining factors, and lessons for future response*, J. Infect. Public Health **13** (2020), no. 7, 956–962, DOI: https://doi.org/10.1016/j.jiph.2020.03.014.
[29] J. P. Schmidt, A. Park, A. Kramer, B. Han, L. Alexander, and J. Drak, *Spatiotemporal fluctuations and triggers of Ebola virus spillover*, Emerg. Infect. Dis. **23** (2017), no. 3, 415–422, DOI: https://doi.org/10.3201/eid2303.160101.
[30] K. Alexander, C. E. Sanderson, M. Marathe, B. L. Lewis, C. M. Rivers, J. Shaman, et al., *What factors might have led to the emergence of Ebola in West Africa?*, PLoS. Negl. Trop. Dis. **9** (2015), no. 6, e0003652, DOI: https://doi.org/10.1371/journal.pntd.0003652.
[31] WHO, *Ebola, West Africa, March 2014–2016*, https://www.who.int/emergencies/situations/ebola-outbreak-2014-2016-West-Africa.
[32] WHO, *Pakistan receives first consignment of COVID-19 vaccines via COVAX Facility*, https://www.emro.who.int/media/news/pakistan-receives-first-consignment-of-covid-19-vaccines-via-covax-facility.html.
[33] A. Nasir, U. B. Aamir, A. Kanji, A. Samreen, Z. Ansar, and N. K. Ghanchi, et al., *SARS-CoV-2 variants of concern (VOC) alpha, beta, gamma, delta, and omicron coincident with consecutive pandemic waves in Pakistan*, medRxiv preprint: DOI: https://doi.org/10.1101/2022.05.19.22275149.
[34] https://www.worldometers.info/coronavirus/country/pakistan/.
[35] D. Kiouach and Y. Sabbar, *The long-time behaviour of a stochastic SIR epidemic model with distributed delay and multidimensional Lévy jumps*, Int. J. Biomath. **15** (2022), no. 3, 2250004, DOI: https://doi.org/10.1142/S1793524522500048.
[36] D. Kiouach and Y. Sabbar, *Dynamic characterization of a stochastic SIR infectious disease model with dual perturbation*, Int. J. Biomath. **14** (2021), no. 4, 2150016, DOI: https://doi.org/10.1142/S1793524521500169.
[37] Y. Sabbar, D. Kiouach, S. P. Rajasekar, S. E. A. El-idrissi, *The influence of quadratic Lévy noise on the dynamic of an SIC contagious illness model: New framework, critical comparison and an application to COVID-19 (SARS-CoV-2) case*, Chaos Solitons Fractals **159** (2022), 112110, DOI: https://doi.org/10.1016/j.chaos.2022.112110.
[38] Y. Sabbar, M. Izadi, A. Raezah, and W. Adel, *Nonlinear dynamics of a general stochastic SIR model with behavioural and physical changes: analysis and application to zoonotic tuberculosis*, Mathematics **12** (2024), no. 13, 1974, DOI: https://doi.org/10.3390/math12131974.